Journal of Crystal Growth 548 (2020) 125848

Contents lists available at ScienceDirect

Journal of Crystal Growth

journal homepage: www.elsevier.com/locate/jcrysgro

GaAs epitaxial growth on R-plane sapphire substrate

Samir K. Saha[a], Rahul Kumar[b,*], Andrian Kuchuk[b], Hryhorii Stanchu[b], Yuriy I. Mazur[b], Shui-Qing Yu[c], Gregory J. Salamo[a,b]

[a] Department of Physics, University of Arkansas, Fayetteville, AR 72701, USA
[b] Institute for Nanoscience and Engineering, University of Arkansas, Fayetteville, AR 72701, USA
[c] Department of Electrical Engineering, University of Arkansas, Fayetteville, AR 72701, USA

ARTICLE INFO

Communicated by H. Asahi

Keywords:
A3. Molecular beam epitaxy
B1. Dissimilar materials
B1. Sapphire
B1. GaAs
A1. High resolution X-ray diffraction
A1. Twinning

ABSTRACT

Achieving epitaxial growth of III-As on r-plane sapphire would potentially allow the integration of both laser and amplifier with corresponding RF electronics. Here we report on the growth of high-quality GaAs on an r-plane sapphire substrate by molecular beam epitaxy. The epitaxial relationship between GaAs and r-plane sapphire is observed and explained. GaAs on r-plane sapphire resulted in (1 1 1) orientation, similar to growth orientation observed on c-plane sapphire. However, in comparison with growth of GaAs growth on a c-plane sapphire substrate, a stronger interaction is observed between GaAs on r-plane sapphire. The effect of growth temperature is also investigated for GaAs growth on r-plane sapphire. It is found that GaAs island size, density, and orientation can be tuned by varying the growth temperature. Finally, a thin AlAs nucleation layer on r-plane sapphire has been introduced to study its effect on the growth of GaAs. The introduction of the AlAs nucleation layer is found to enhance the wetting of GaAs but at the expense of introducing twinning defects.

1. Introduction

GaAs and AlAs on sapphire are excellent candidates for microwave photonics, optoelectronics and electronics owing to a thermal expansion coefficient match and a large refractive index contrast between the two materials [1]. An additional attractive quality of the sapphire substrate is its large bandgap (~9 eV) resulting in excellent resistance to radiation damage, making it a candidate for space and nuclear-related applications [2]. In fact, r-plane ($1\bar{1}02$) sapphire, as a substrate, is an ideal platform for integrated RF electronics and already the choice for silicon on sapphire (SOS) technology. While there are a few reports of epitaxial growth of cubic Si(Ge) on both c and r plane sapphire [3–6] and cubic III-As on c-plane sapphire [1,7–12], to the best of our knowledge, there are no reports about epitaxial growth of III-As on r-plane sapphire as a substrate. Achieving epitaxial growth of III-As on r-plane sapphire would potentially allow the integration of both laser and amplifier with corresponding RF electronics.

Heteroepitaxy normally combines two different materials having a similar crystal structure and most often results in epitaxial films having the same orientation as of the substrate. However, for the heteroepitaxial material system of GaAs on sapphire we have a combination of dissimilar material systems. Consequently, it is not trivial to grow nor predict the orientation and quality of the GaAs film. For example, for the growth of GaAs on r-plane sapphire, the rectangular (1 1 0) plane of GaAs may align with the rectangular r-plane of sapphire, while the hexagonal nature of the sapphire substrate might force the epitaxial growth of GaAs to be of (1 1 1) orientation, or GaAs might take a totally different orientation. Here we report on an investigation of the epitaxial growth of III-As on r-plane ($1\bar{1}02$) sapphire.

The epitaxial orientation and the correlation between film and substrate are certainly important and can have an impact on both the optical and carrier transport properties of GaAs structures. To understand the possible orientations for GaAs on r-plane sapphire, the atomic arrangement of the r-plane of sapphire, the (1 1 1) plane and (1 1 0) plane of GaAs are shown together in Fig. 1. The lattice mismatch has been calculated considering each different potential alignment shown. For example, for the case of the GaAs (1 1 1) crystal plane the compressive strain for GaAs on sapphire is 35.2% and the tensile strain is 16.2%, in the two perpendicular directions. On the other hand, for the (1 1 0) crystal plane, it has compressive strain (10.7%) and tensile strain (16.2%).

While the lattice mismatch is very important, the substrate surface energy also plays an important role in deciding the orientation and quality of the epitaxial growth of GaAs on sapphire. For example, for layer-by-layer growth of epitaxial GaAs material, the energy dynamics at the surface plays a role through the relationship:

$$\gamma_s \geq \gamma_i + \gamma_e \quad (1)$$

* Corresponding author.

https://doi.org/10.1016/j.jcrysgro.2020.125848
Received 3 August 2020; Received in revised form 19 August 2020; Accepted 21 August 2020
Available online 27 August 2020

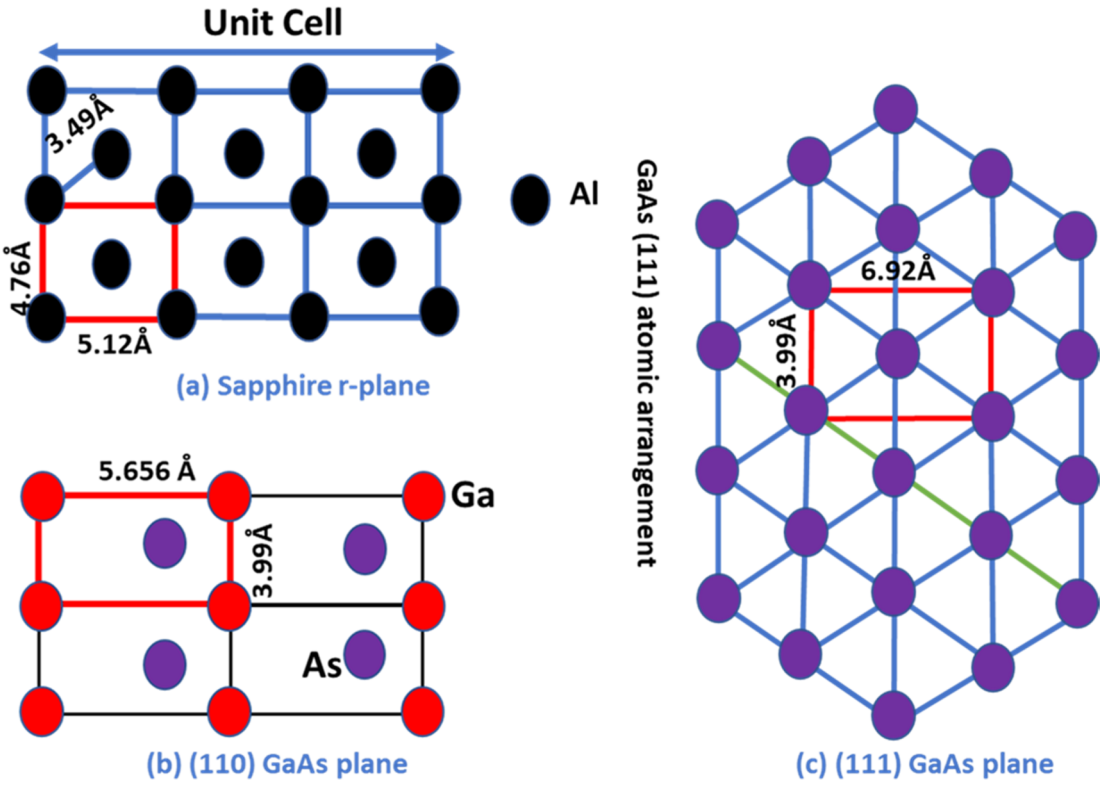

Fig. 1. Atomic arrangement of (a) r-plane sapphire, (b) GaAs (1 1 0) plane, and (c) GaAs (1 1 1) plane.

where γ_s is substrate surface energy, γ_i is interface energy between substrate and film, and γ_e is film surface energy. The surface energy of relaxed c-plane and r-plane is 1.85 and 2.26 Jm^{-2} respectively [13]. Interestingly, the higher surface energy of r-plane sapphire over c-plane sapphire favors a better film to substrate interaction in the case of GaAs growth on an r-plane sapphire substrate. With this difference in mind, we investigated the growth of GaAs on sapphire by (i) comparing growth on c-plane and r-plane substrates, (ii) investigating the effect of growth parameters on the material morphology, and (iii) probing the effect of an AlAs nucleation layer on the growth of GaAs on r-plane sapphire.

2. Experimental procedure

A Riber-32 molecular beam epitaxy (MBE) chamber was used to grow all the samples. Substrates were back side coated with 1-μm thick Ti for efficient and uniform radiative heating from the heater [14]. Substrates were introduced into the load lock chamber and heated at 200 °C for one hour to evaporate water vapor from the substrate surface. Afterward, substrates were annealed at 900 °C for 6 h in the degassing chamber to remove organic contaminants and then transferred to the MBE growth chamber, all under vacuum. In the growth chamber, the surface of each substrate was exposed to an arsenic flux of 2×10^{-6} torr at 650 °C for half an hour [15], after which the substrate temperature was set to the growth temperature. All temperatures mentioned in this work are the thermocouple temperature reading, which is not in touch with the substrate so there can be as much as a 50 °C temperature difference between the thermocouple reading and the actual surface temperature during growth. The growth rates for GaAs and AlAs were 0.75 and 0.2 ML/s, respectively. To study the growth in real-time, reflection high energy electron diffraction (RHEED) was used at 20 keV accelerating voltage and 1.5A cathode current at a glancing angle of 1-2° to the substrate.

The surface morphology, after growth, for each sample was investigated using the intermittent contact mode of atomic force microscopy (AFM) (Bruker, model number 3000 dimension III). A silicon tip with radius 10 nm was used in the AFM to image samples under equilibrium conditions and using optimized feedback and force parameters. X-ray diffraction (XRD) was used to determine the epitaxial orientation and crystal quality of the substrate and films. The XRD instrument was equipped with a multilayer focusing mirror and a Cu Kα1 source of radiation with wavelength 1.54 Å.

3. Results and discussion

All sapphire substrates, used in this work, possessed a well-defined starting step-terrace surface. The importance of having a step-terrace and clean substrate surface for dissimilar material growth is shown elsewhere [1,16]. These surfaces were achieved by heating as-received substrates at 1200 °C for 6 h in atmospheric conditions. Fig. 2 shows the representative AFM images of a c-plane and an r-plane sapphire substrate. For the c-plane sapphire substrate, the average step height is 0.22 nm, which corresponds to 1 monolayer (ML) of c-plane sapphire with an average terrace width of 236 nm.

On the other hand, the average step height and terrace width of r-plane sapphire was 0.76 nm and 198 nm, respectively. The difference is also due to the unintentional miscut of the r-plane substrate (0.2°), which was higher than the c-plane substrate (0.06°). The RHEED pattern for both surfaces is shown in the inset of both images. Narrow streaks, and the presence of Kikuchi lines, confirm the cleanliness of the substrate surfaces.

(a) Comparison of GaAs growth on c and r-plane sapphire:

GaAs was grown directly on c-plane (sample: C-600) and r-plane sapphire (sample: R-600) after substrate preparation. 10 nm GaAs were deposited on both substrates at 600 °C under identical growth conditions. Thickness values were calibrated for homoepitaxial GaAs (1 0 0) growth. AFM surface morphologies of both samples are shown in Fig. 3(a) and (b). Both images show GaAs three-dimensional (3D)

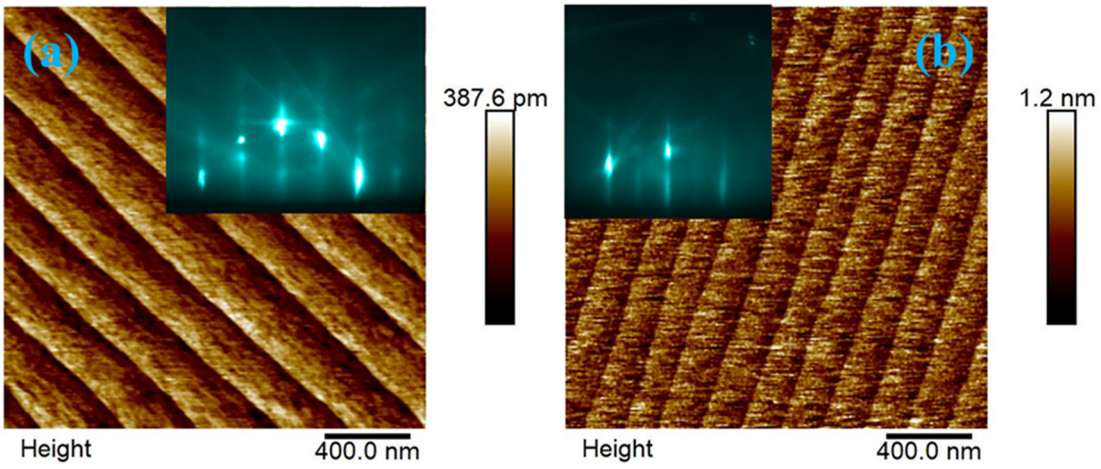

Fig. 2. AFM images of c-plane (a) and r-plane (b) sapphire substrates. Inset shows the substrate RHEED just before the growth.

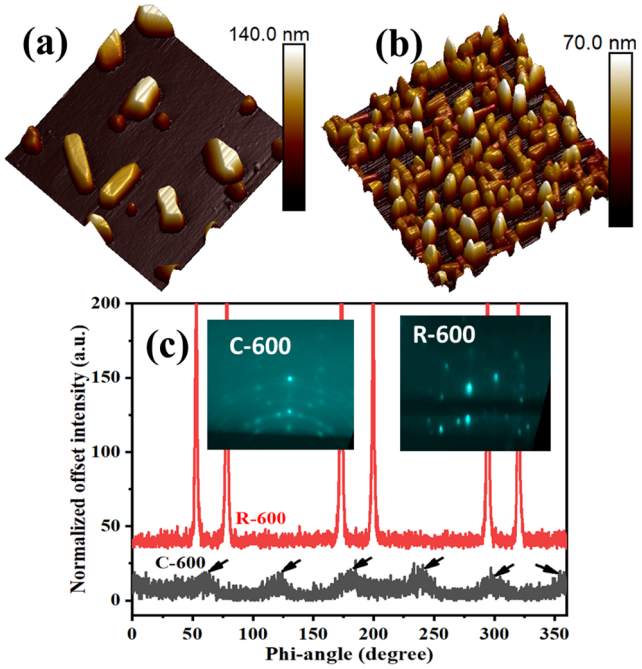

Fig. 3. AFM Surface morphology on 2 μm × 2 μm scan area of 10 nm GaAs growth on (a) c-plane (C-600) and (b) r-plane sapphire substrate (R-600); (c) Phi-scans of both samples, arrows (red for R-600 and black for C-600) showing GaAs (220) peaks, corresponding RHEED images after the growth are shown in the inset of figure.

Table 1
Island height, density, and total volume on 2 μm × 2 μm AFM scan area.

Sample ID	Average height (nm)	Density (cm^{-2})	Volume of 3D islands (m^3)
C-600	85	4.25×10^{8}	4×10^{-20}
R-600	40	4.35×10^{9}	4.3×10^{-20}

islands, indicating a 3D growth mode. 3D island size, density, and volume of GaAs material deposited are listed in Table 1 for a 2 μm × 2 μm scanned area. In both cases, 3D islands are observed. High lattice mismatch and dissimilar crystal structure in both cases promote 3D growth. Since the surface energy of r-plane sapphire is higher than the c-plane sapphire, the interaction of GaAs on the r- plane should be higher than the c-plane sapphire substrate, which increased the density of GaAs islands in r-plane. Basically, diffusion and ripening are slower on r-plane.

Fig. 3(c) shows the GaAs (220) phi-scans of both samples. All GaAs (220) peaks of C-600 are shown with arrows. GaAs peaks in R-600 are very sharp, whereas peaks are broad in C-600. This sharp peak shows a well-defined in-plane correlation in R-600 as opposed to C-600 where the in-plane correlation with the substrate is very weak. Moreover, phi-scan shows six-fold symmetry for C-600, indicating the presence of 60° rotated twins. Six peaks corresponding to GaAs (220) can also be observed in R-600, but these peaks are not exactly separated by 60°. This shows that there are two different domains of [111] oriented crystals, and these two domains are maintaining two different in-plane crystallographic orientation relationships with the r-plane sapphire substrate. The equal intensity of both types of peaks shows that both orientation relationships are equally preferable. RHEED images after GaAs growth from C-600 and R-600 are shown in the inset of Fig. 3(c). For C-600, RHEED shows spots and rings. The spotty pattern indicates the 3-D growth mode, whereas the ring pattern indicates the weak in-plane correlation between substrate and GaAs which agrees with the XRD result. On the other hand, for the r-plane (R-600), spots without a ring pattern was observed. This again shows the better interaction and well-defined GaAs orientation relationship of r-plane sapphire than with the c-plane sapphire substrate. All results are consistent with expectations based on Eq. (1).

XRD omega-2theta scans of both samples are shown in Fig. 4. For C-600, only a GaAs (111) orientation is detected, whereas (111) and

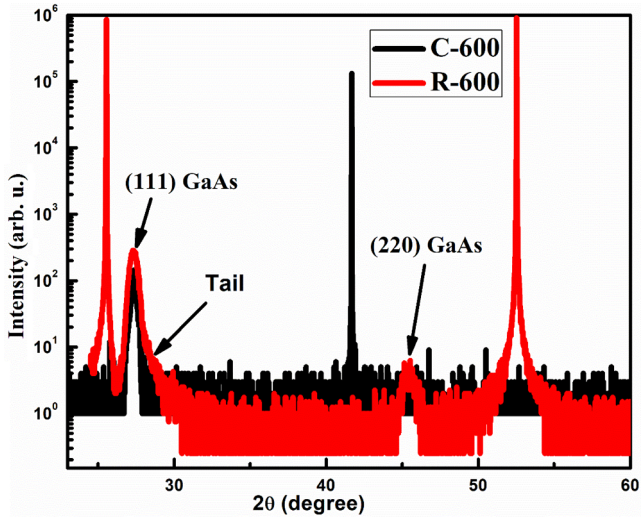

Fig. 4. XRD omega-2theta scan of C-600 and R-600. Sharp and intense peaks are related to sapphire substrates.

(1 1 0) orientations are detected for R-600. A higher angle tail in the GaAs (1 1 1) peak for R-600 is also observed, perhaps due to the strain difference in the two orientations of GaAs observed in phi-scan.

(b) Effect of growth temperature on GaAs/r-plane sapphire:

There are a number of parameters that can affect the surface morphology and crystal quality of the grown materials, such as growth temperature, growth rate, the ratio of V/III beam flux, and the substrate surface [1,17]. To investigate the effect of growth temperature, four different temperatures 500 °C (R-500), 600 °C (R-600), 650 °C (R-650) and 700 °C (R-700) were used to grow 10 nm of GaAs on the r-plane sapphire substrate. The study of growth temperature effects of GaAs growth on c-plane sapphire is discussed in our previous work [1]. For GaAs on the r-plane, growth at 700 °C resulted in no detectable deposition of GaAs. AFM, RHEED and X-ray photoelectron spectroscopy (XPS) show no signature of GaAs or metallic Ga deposition. Apparently, the growth temperature is too high for any appreciable sticking of either Ga or As adatoms. However, GaAs was deposited, and the surface morphology and crystal quality were investigated, at 500 °C, 600 °C, and 650 °C. Fig. 5 shows the surface morphologies for these three samples.

R-500 (Fig. 5a) has the best surface coverage by GaAs islands. GaAs island size increases with increasing growth temperature while the island density decreases with GaAs growth temperature (see Table 2). These observations are consistent with ripening [18,19]. From the RHEED images, R-500 sample RHEED shows the ring pattern, which indicates a weak in-plane correlation between the film and the substrate. With increasing temperature, however, for both R-600 and R-650, the ring pattern vanishes, and a spotty pattern becomes prominent. Twinning can also be seen in RHEED images for R-600 and R-650.

Omega-2theta scans of these three samples are shown in Fig. 6(a). Only the (1 1 1) orientation was observed for R-500 and R-650. Meanwhile, the R-600 sample shows the presence of two orientations: (1 1 1) and (1 1 0). Fig. 6(b) shows the phi-scans of GaAs (2 2 0) plane for (1 1 1) orientation. The orientation relationship remains unchanged with the variation of growth temperature. It is also noticeable from the phi scan that a higher temperature helps to improve the in-plane correlation. For the low -temperature sample (R-500), the phi peaks are broad and diffuse, which indicates the weak in-plane correlation, and this result is also in agreement with RHEED. The phi peaks for both samples (R-600, R-650) are sharp and well defined, so the high temperature is necessary for a better in-plane correlation between epitaxial GaAs films and substrates.

Table 2
Growth temperature, GaAs island height and density for three GaAs/r-plane sapphire samples.

Sample ID	Growth temperature (°C)	Height (nm)	Density (/cm^2)
R-500	500	9	NA
R-600	600	40	4.35×10^9
R-650	650	52.6	3.4×10^9

(a) Introduction of AlAs layer:

Since GaAs does not wet the sapphire surface very well, we investigated adding a thin AlAs buffer layer on r-plane sapphire before adding GaAs. This was motivated by our earlier work that showed that a thin AlAs layer improved the chemical interaction and hence, the quality of subsequent GaAs thin films on c-plane sapphire [1]. Therefore, after adding a thin AlAs layer on sapphire, GaAs was grown under three different arsenic flux conditions: 1×10^{-6} (RA-1), 3.5×10^{-6} (RA-3.5) and 6×10^{-6} (RA-6). For these samples, the GaAs growth temperature was held at 600 °C. Fig. 7 shows the AFM surface morphologies of these samples. For all three samples, highly dense 3D islands are observed. The surface roughness of these samples is increased with increasing arsenic pressure, and the roughness values are 2.53 nm (RA-1), 2.86 nm (RA-3.5), and 3.68 nm (RA-6). While comparing these surfaces to the samples where GaAs were directly grown on sapphire (R-500, R-600, and R-650), we can see that adding a thin AlAs layer does improve the wetting the sapphire substrate with GaAs, similar to our observation on c-plane sapphire 1. The Al-O (502 kJ/mol) bond is stronger compared to the Ga-O (374 kJ/mol) and the As-O (374 kJ/mol) bonds [20]. Stronger bonding at the interface will reduce the interface energy. Hence, improved wetting after introduction of AlAs is consistent with Eq. (1).

Fig. 8(a) shows the omega-2theta scan of these three samples. Only GaAs (1 1 1) orientation was observed. Here we observe a clear peak beside the GaAs (1 1 1) peak towards the higher angle side instead of a tail that was observed for direct growth of GaAs on r-plane sapphire. This peak corresponds to a high tensile strain for GaAs/AlAs material. Fig. 8(b) shows the phi-scans of these samples and r plane sapphire.

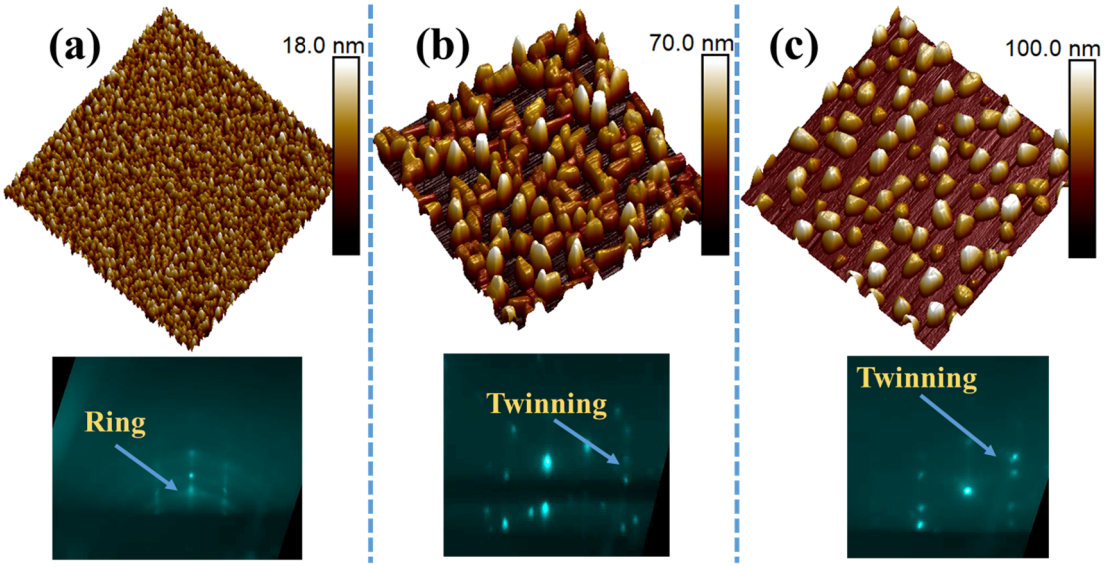

Fig. 5. AFM and RHEED of (a) R-500 (b) R-600 (c) R-650.

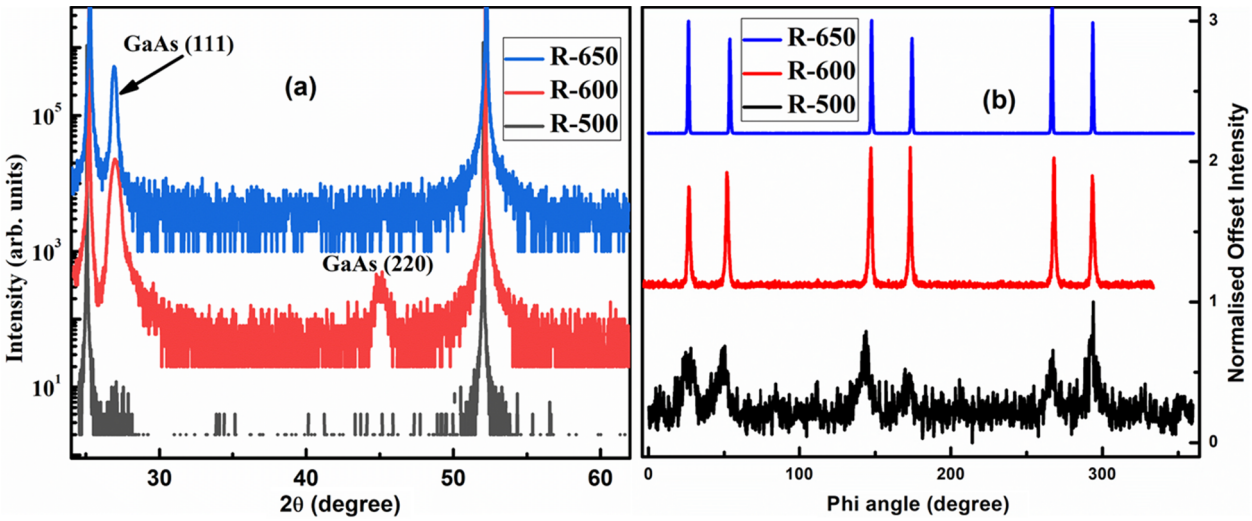

Fig. 6. (a) Omega-2theta scan, and (b) phi-scan of R-500, R-600 and R650.

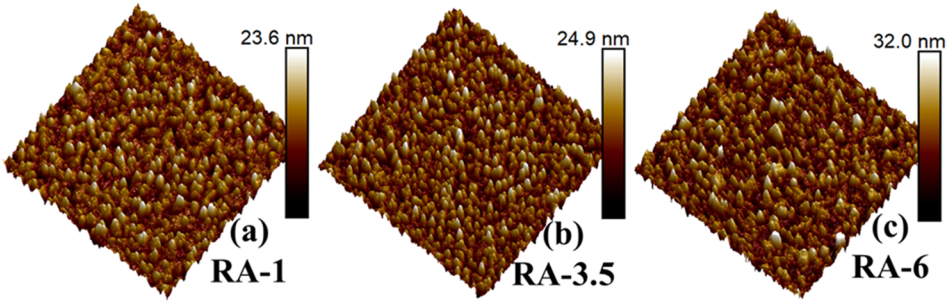

Fig. 7. AFM surface morphology of (a) RA-1 (b) RA-3.5 (c) RA-6.

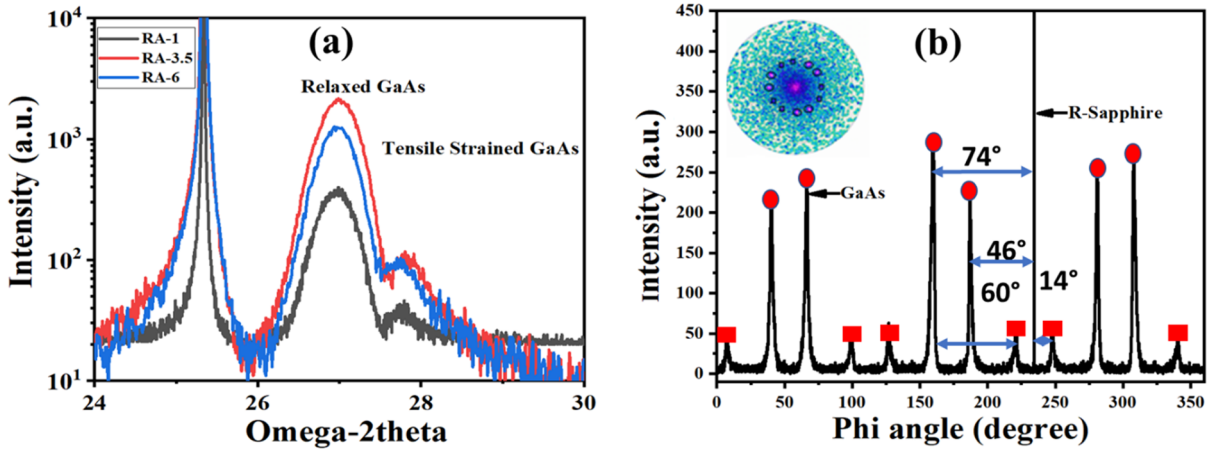

Fig. 8. (a) Omega-2theta scan and (b) phi-scan of RA-1, twin peaks are denoted by rectangles, angles between different types of peaks are shown in the figure. Pole figure of the same sample is shown in the inset with sample tilt ranging from 0 to 70°.

In the zinc blende system, the phi-scan of the 220 reflection shows three equally separated peaks, which represent three-fold symmetry. In the presence of 60° twins, it shows six equally separated peaks. However, here we observe 12 different 220 peaks, which is unusual for a cubic zinc blende system (shown in Fig. 8b). This is due to two major orientations, which are shifted by approximately ± 14° with respect to the 0006 reflection of the r-plane sapphire. Both orientations have their 60° twin peaks, which makes a total of 12 (220) peaks. The two orientations are depicted in Fig. 9 by two hexagons O1 and O2. Atomic distances are to the scale with small error. These two orientations of the 110 axis of GaAs make an angle of approximately ± 14° with respect to the [100] in-plane direction of r-plane sapphire.

It is possible that initially, with smaller coverage of GaAs, only one orientation of GaAs existed where [100] in-plane direction of sapphire was aligned to [110] in-plane direction of GaAs. In other words, GaAs hexagon was sitting on seed hexagon (shown by green dashed lines in

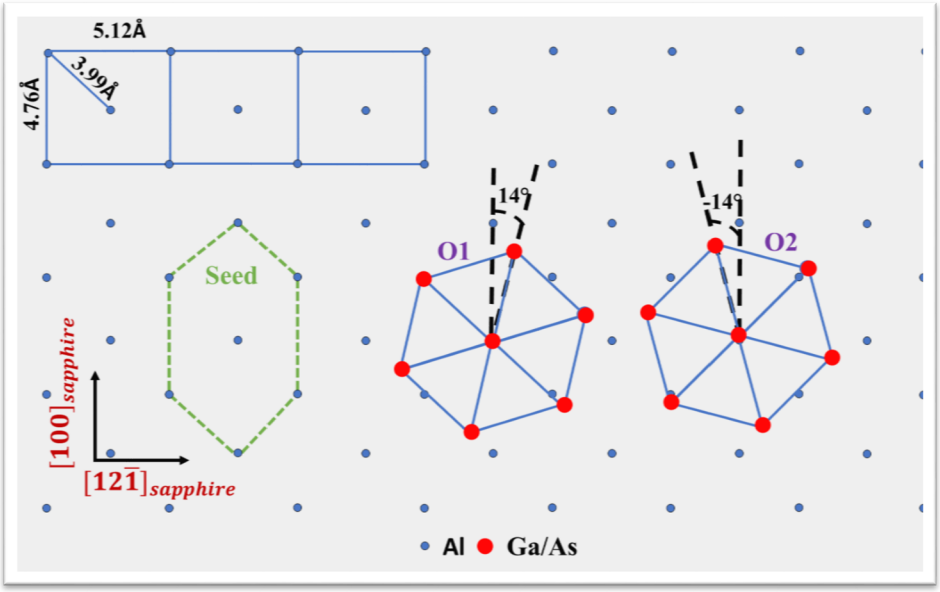

Fig. 9. Arrangement of Al atoms in r plane sapphire (blue dots) and two possible in-plane orientations of GaAs separated by approximately 28°.

Fig. 9). As the coverage of GaAs increases, the strain also increases, and initial orientation split in two orientation O1 and O2 by a 14° twist to minimize the strain.

4. Conclusion

A highly dissimilar material system of GaAs on r-plane sapphire has been grown. It has been compared with GaAs on c-plane sapphire. The role of growth temperature and the addition of an AlAs nucleation layer on GaAs epitaxial films were investigated. Due to the higher surface energy of r-plane sapphire, the interaction between GaAs films and r-plane sapphire is better than c-plane sapphire. Two in-plane correlations are observed for GaAs films with r -plane sapphire, which is ~28° apart, irrespective of growth temperatures. The AlAs nucleation layer enhances the wetting of GaAs films on r-plane sapphire substrates; however, twinning defects are also observed. We are optimistic that a two-step growth method, with annealing, will result in a quality GaAs surface as demonstrated for GaAs on c-plane sapphire.

CRediT authorship contribution statement

Samir K. Saha: Data curation, Methodology, Investigation. **Rahul Kumar:** Investigation, Visualization, Writing - original draft. **Andrian Kuchuk:** Data curation. **Hryhorii Stanchu:** Formal analysis. **Yuriy I. Mazur:** Project administration. **Shui-Qing Yu:** Conceptualization, Funding acquisition. **Gregory J. Salamo:** Writing - review & editing, Conceptualization, Funding acquisition.

Declaration of Competing Interest

The authors declare that they have no known competing financial interests or personal relationships that could have appeared to influence the work reported in this paper.

Acknowledgments

The authors acknowledge the financial support by the Institute for Nanoscience and Engineering, University of Arkansas, and the project "Quantum Interfaces of Dissimilar Materials" funded by National Science Foundation(NSF) (Grant No. 1809054). Additionally, Dr. Shui-Qing Yu would also like to acknowledge the NSF funding support ECCS1745143.

References

[1] S.K. Saha, R. Kumar, A.V. Kuchuk, M.Z. Alavijeh, Y. Maidaniuk, Y.I. Mazur, S.-Q. Yu, G.J. Salamo, Cryst. Growth Des. 19 (2019) 5088.
[2] S. Ebnesajjad, S. Ebnesajjad, in: Surf. Treat. Mater. Adhes. Bond, second ed., William Andrew Publishing, 2014, pp. 283–299.
[3] H.J. Kim, Y. Park, H. Bin Bae, S.H. Choi, Adv. Condens. Matter Phys. (2015, 2015,) 1.
[4] H.J. Kim, H. Bin Bae, Y. Park, K. Lee, S.H. Choi, J. Cryst. Growth 353 (2012) 124.
[5] Y. Park, G.C. King, S.H. Choi, J. Cryst. Growth 310 (310) (2008) 2724.
[6] W. Dubbelday, K. Kavanagh, J. Cryst. Growth 222 (2001) 20.
[7] A. Sugimura, T. Hosoi, K. Ishibitsu, T. Kawamura, J. Cryst. Growth 77 (1986) 524.
[8] K. Kasai, K. Nakai, M. Ozeki, J. Appl. Phys. 60 (1986) 1.
[9] T.P. Humphreys, C.J. Miner, J.B. Posthill, K. Das, M.K. Summerville, R.J. Nemanich, C.A. Sukow, N.R. Parikh, Appl. Phys. Lett. 54 (1989) 1687.
[10] T.P. Humphreys, C.J. Miner, N.R. Parikh, K. Das, M.K. Summerville, J.B. Posthill, R.J. Nemanich, C.A. Sukow, MRS Proc. 144 (1988) 195.
[11] T.F. Kuech, A. Segmüller, T.S. Kuan, M.S. Goorsky, J. Appl. Phys. 67 (1990) 6497.
[12] L.C. Chuang, M. Moewe, K.W. Ng, T.-T.-D. Tran, S. Crankshaw, R. Chen, W.S. Ko, C. Chang-Hasnain, Appl. Phys. Lett. 98 (2011) 123101.
[13] T. Stirner, J. Sun, M. Aust, Phys. Procedia 32 (2012) 635.
[14] V. Petukhov, A. Bakin, I. Tsiaoussis, J. Rothman, S. Ivanov, J. Stoemenos, A. Waag, J. Cryst. Growth 323 (2011) 111.
[15] C.J.M.T.P. Humphreys, N.R. Parikh, K. Das, J.B. Posthill, R.J. Nemanich, M.K. Summerville, C.A. Sukow, J. Chem. Inf. Model. 53 (2013) 1689.
[16] H.J. Kim, A. Duzik, S.H. Choi, Acta Mater. 145 (2018) 1.
[17] L. Esposito, S. Bietti, A. Fedorov, R. Nötzel, S. Sanguinetti, Phys. Rev. Mater. 1 (2017) 024602.
[18] G. Madras, B.J. McCoy, J. Chem. Phys. 119 (2003) 1683.
[19] T.V. Western, R. Groot, Cryst. Growth Des. 18 (2018) 4952.
[20] Y.-R. Luo, Y.-R. Luo, Comprehensive Handbook of Chemical Bond Energies, CRC Press, 2007.